Imaging Brain Amyloid in Alzheimer's Disease with Pittsburgh Compound-B

William E. Klunk, MD, PhD,[1] Henry Engler, MD,[2] Agneta Nordberg, MD, PhD,[3,4] Yanming Wang, PhD,[5] Gunnar Blomqvist, PhD,[2] Daniel P. Holt, BS,[5] Mats Bergström, PhD,[2] Irina Savitcheva, MD,[2] Guo-feng Huang, PhD,[5] Sergio Estrada, PhD,[2] Birgitta Ausén, MSCI,[4] Manik L. Debnath, MS,[1] Julien Barletta, BS,[6] Julie C. Price, PhD,[5] Johan Sandell, PhD,[2] Brian J. Lopresti, BS,[5] Anders Wall, PhD,[2] Pernilla Koivisto, PhD,[2] Gunnar Antoni, PhD,[2] Chester A. Mathis, PhD,[5] and Bengt Långström, PhD[2,6]

This report describes the first human study of a novel amyloid-imaging positron emission tomography (PET) tracer, termed Pittsburgh Compound-B (PIB), in 16 patients with diagnosed mild AD and 9 controls. Compared with controls, AD patients typically showed marked retention of PIB in areas of association cortex known to contain large amounts of amyloid deposits in AD. In the AD patient group, PIB retention was increased most prominently in frontal cortex (1.94-fold, $p = 0.0001$). Large increases also were observed in parietal (1.71-fold, $p = 0.0002$), temporal (1.52-fold, $p = 0.002$), and occipital (1.54-fold, $p = 0.002$) cortex and the striatum (1.76-fold, $p = 0.0001$). PIB retention was equivalent in AD patients and controls in areas known to be relatively unaffected by amyloid deposition (such as subcortical white matter, pons, and cerebellum). Studies in three young (21 years) and six older healthy controls (69.5 ± 11 years) showed low PIB retention in cortical areas and no significant group differences between young and older controls. In cortical areas, PIB retention correlated inversely with cerebral glucose metabolism determined with 18F-fluorodeoxyglucose. This relationship was most robust in the parietal cortex ($r = -0.72$; $p = 0.0001$). The results suggest that PET imaging with the novel tracer, PIB, can provide quantitative information on amyloid deposits in living subjects.

Ann Neurol 2004;55:306–319

We and others have worked to develop in vivo amyloid-imaging agents for use with a variety of brain imaging techniques.[1–8] Modification of the amyloid-binding histological dye, thioflavin-T, led to the finding that neutral benzothiazoles bound to amyloid with high affinity and crossed the blood–brain barrier very well.[5] The basic properties of the prototypical benzothiazole amyloid binding agent 2-(4′methylaminophenyl)benzothiazole (termed *BTA-1*) and related derivatives have been described in detail.[8–10] These studies showed that these compounds could bind to amyloid with low nanomolar affinity, enter brain in amounts sufficient for imaging with positron emission tomography (PET), and clear rapidly from normal brain tissue. At the low nanomolar concentrations typically used in PET studies, the binding of BTA-1 to postmortem human brain was shown to be a good indication of Aβ amyloid deposition but did not appear to detect the presence of neurofibrillary tangles.[11] The exact form of the amyloid target of BTA-1 binding have not yet been identified with certainty. In vitro studies[11] suggest that BTA-1 binds to aggregated, fibrillar Aβ deposits such as those found in the cortex and striatum, but not to the amorphous Aβ deposits such as those that predominate in cerebellum. The binding of BTA-1 and related derivatives to oligomeric Aβ has not yet been studied.

A structure-activity study of a series of benzothiazoles suggested that a hydroxylated BTA-1 derivative had brain clearance properties typical of many useful PET radiotracers.[10] Therefore, this hydroxybenzothiazole was chosen as the lead compound for the first human trial of benzothiazole amyloid-imaging agents. For simplicity, the compound, *N*-methyl-[^{11}C]2-(4′-methylaminophenyl)-6-hydroxybenzothiazole, was given the Uppsala University PET Centre code of "Pittsburgh Compound-B" or, simply, PIB. Preclinical studies showed that PIB bound to Alzheimer's disease (AD) brain with a K_d of 1 to 2nM, entered the brain rapidly (approximately 7%ID/g 2 minutes after intravenous in-

From the [1]Department of Psychiatry, University of Pittsburgh, Pittsburgh, PA; [2]Uppsala University, PET Centre/Uppsala Imanet AB, Uppsala; [3]Neurotec Department, Karolinska Institute, Huddinge University Hospital, Stockholm; [4]Department of Geriatric Medicine, Huddinge University Hospital, Stockholm, Sweden; [5]Department of Radiology, PET Facility, University of Pittsburgh, Pittsburgh, PA; and [6]Department of Organic Chemistry, Uppsala University, Uppsala, Sweden.

Received Sep 9, and in revised form Nov 4, 2003. Accepted for publication Nov 18, 2003.

Address correspondence to Dr Mathis, PET Facility, B-938 UPMC Presbyterian, 200 Lothrop Street, Pittsburgh, PA 15213-2582.
E-mail: mathisca@upmc.edu

jection in mice), and cleared rapidly from normal mouse brain (clearance $t_{1/2}$ approximately 8 minutes).[10] Using real-time in vivo multiphoton microscopy, researchers have shown that PIB and other benzothiazole amyloid-imaging agents label individual amyloid plaques in transgenic mouse models of AD within 3 minutes after intravenous injection and clear rapidly from normal brain parenchyma.[8,12] This study describes the first results from PIB PET imaging of 16 mild AD patients and 9 healthy control (HC) subjects.

Subjects and Methods

Preclinical development of the benzothiazole class of compounds and PIB was completed at the University of Pittsburgh,[10] recruitment and evaluation of AD patients subjects and older controls were performed at the Department of Geriatric Medicine, Huddinge University Hospital, and good manufacturing process evaluation of PIB and human PET studies were performed at Uppsala University.

PET-Microdosing Toxicology

The human use of PIB was preceded by a toxicity assessment using the PET-microdosing concept.[13] Toxicological studies included genotoxicity (chromosomal aberration, mouse lymphoma mutagenesis, bacterial reverse mutation assay, and mouse micronucleus assay), single dose toxicity in rats, and cardiopulmonary physiology in the rhesus monkey. No toxic effects of PIB were observed.

Radiotracers

^{18}F-fluorodeoxyglucose (^{18}FDG) and PIB were produced according to the standard good manufacturing process at the Uppsala University PET Centre. PIB, *N*-methyl-[^{11}C]2-(4′-methylaminophenyl)-6-hydroxybenzothiazole, was prepared (Fig 1) by the method described previously,[10] with several modifications including the use of NaH as base and dimethyl formamide as the reaction solvent. A solution of PIB consisting of normal saline (2ml), propyleneglycol (2ml), ethanol (0.7ml), and HCl (0.3mM) was filtered (Dynagard ME, 0.22μm), yielding a solution that was sterile and apyrogenic. Addition of 5ml sterile phosphate-buffered saline to the solution adjusted the pH to between 6.0 and 7.0. The radiochemical yield was in the range of 10 to 15% based on [^{11}C]methyl iodide, and the specific radioactivity was on average 25GBq/μmol (range, 6–74) at end of synthesis. Routine quality control of the solutions for human injection consisted of a pH measurement and high-performance liquid chromatography analysis to determine radiochemical and chemical purity. The radiochemical purity was greater than 95%. In addition, the following analyses were performed on selected batches: sterility and endotoxin test, radiochemical and chemical stability test including column recovery determination, and verification of the identity of the radiolabeled compound with liquid chromatography mass spectrometry.

Autoradiography

Fresh-frozen pieces (2 × 2cm) of frontal cortex from postmortem brain of Alzheimer's patients and from age-matched control brain were used for the autoradiographic binding studies. Tissue was obtained from the University of Pittsburgh Alzheimer Disease Research Center Brain Bank and was collected as previously described.[11] Frozen sections (25μm) were preincubated in phosphate-buffered saline, pH 7.0, complemented with 2% bovine serum albumin, for 8 to 10 minutes. Subsequently, the sections were incubated in 10nM PIB, with or without 10μM BTA-1 (unlabeled compound) for 30 minutes, in the same buffer. After that, the slices were washed 2 × 2 minutes in the same buffer with an additional 2 × 2–minute wash step in buffer without bovine serum albumin. Finally, the slides were dried under an air stream, at 37°C, for 8 to 10 minutes, before being exposed to β-sensitive phosphor imager plates (Molecular Dynamics, Sunnyvale, CA) for at least 40 minutes. The exposed plates were scanned in a PhosphorImager, model 400S (Molecular Dynamics) and the obtained digital images were displayed and analyzed by the software ImageQuant 5.1 (Molecular Dynamics).

Human Subjects

HEALTHY VOLUNTEERS. Nine subjects volunteered as HCs for the PIB study and for regional cerebral glucose metabolic rate ($rCMR_{glc}$) by ^{18}FDG. Six older controls (OCs) ranging in age from 59 to 77 years old, and three young controls (YCs) all 21 years old were examined. The three YCs were studied under a separate Human Ethics Committee Protocol, which included an arterial line for the purpose of collecting samples for metabolite analysis and input function determination. Arterial sampling was not included in the initial AD patient protocol but subsequently was obtained from three AD patients and two older controls under a modified protocol (see below). In addition to the arterial sampling, the YC subjects also were included because of the near certainty that these young subjects would represent true plaque-negative controls. None of the HC subjects had a history of a medical or neurological disease or substance abuse, and all scored normally on neuropsychological testing.

ALZHEIMER'S DISEASE PATIENTS. Sixteen AD patients (Tables 1 and 2) ranging in age from 51 to 81 years old were

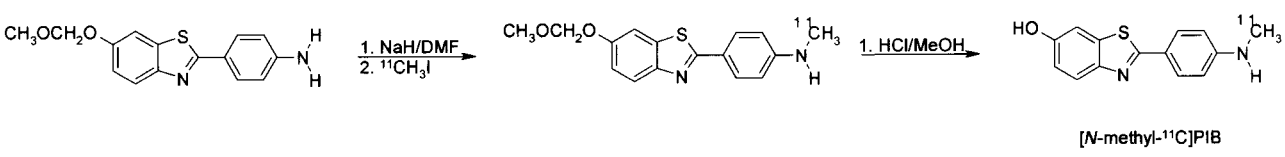

Fig 1. Reaction scheme for the radiochemical synthesis of PIB.

Table 1. Clinical Data of Individual AD Patients

ID[a]	Duration (yr)	MMSE at Diagnosis	Time Since Diagnosis (yr)	MMSE at Study	ChEI	Years Taking ChEI[b]
AD1[c]	4	28	0.5	26	No	0
AD2	6	27[d]	4	25	Yes	3
AD3	2	18	0.2	18	No	0
AD4[e]	**5**	**29**	**4**	**28**	**Yes**	**4**
AD5	6	25	4	22	Yes	4
AD6	7	25	6	21	Yes	4
AD7	5	29	4	18	Yes	4
AD8	1	25	0.3	25	No	0
AD9	3	27	0.3	25	No	0
AD10	4	27	2	25	Yes	2
AD11	5	28	3	27	Yes	2
AD12[e]	**5**	**28**	**3**	**28**	**Yes**	**2**
AD13	4	29	2	27	Yes	2
AD14[e]	**4**	**28**	**2**	**29**	**Yes**	**2**
AD15	4	23[f]	3	27	Yes	3
AD16	4	27	0	27	No	0
Mean	4.3	26.6	2.4	24.9	11 Yes	2.9
SD	1.5	2.9	1.8	3.4	5 No	0.9

[a]AD patient identification code.
[b]Mean treatment time refers to only those receiving ChEI treatment.
[c]AD patient AD1 was not included in standardized uptake value analyses for the reason listed in Results.
[d]The first available MMSE score is from 2 years before the study.
[e]AD4, AD12, and AD14 showed PIB retention typical of that seen in controls.
[f]The first available MMSE score is from 1 year before the study.

AD = Alzheimer's disease; MMSE = Mini-Mental State Examination; ChEI = cholinesterase inhibitor therapy.

Table 2. Group Mean Clinical Data

Parameter	AD	OC	YC
Age (yr)	65.9 ± 10.7	69.0 ± 7.2	21 ± 0
Female	5	3	3
Male	11	3	0
Education (yr)	12.3 ± 3.7	12.7 ± 4.0	n/a[a]
ApoE 3/3	8	nd	nd
ApoE 2/4	1	nd	nd
ApoE 3/4	1	nd	nd
ApoE 4/4	6	nd	nd
CSF Aβ42 <450pg/ml[b]	11 of 16	nd	nd
Mean CSF Aβ42	372 ± 129	nd	nd
CSF tau >400pg/ml[b]	10 of 16	nd	nd
Mean CSF tau	639 ± 283	nd	nd

[a]Because these young volunteers had not yet reached their full educational potential.
[b]Indicates the number of patients with a level outside of the normal range.

AD = Alzheimer's disease; OC = older control; YC = younger control; n/a = not applicable; ApoE = apolipoprotein E; nd = not determined; CSF = cerebrospinal fluid.

recruited at the department of Geriatric Medicine, Huddinge University Hospital, Karolinska Institute. The AD patients had diagnoses of probable AD according to National Institute of Neurological and Communication Disorders Alzheimer's Disease and Related Disorders Association criteria.[14] Before diagnosis, subjects underwent a comprehensive clinical examination including medical history with close informant, neurological and psychiatric examination, routine blood analysis, cerebrospinal fluid analysis for Aβ(1-42) and tau, electrocardiogram, magnetic resonance imaging/computed tomography scans, single-photon emission computed tomography blood flow scans, electroencephalography, apolipoprotein E (ApoE) genotyping, and a comprehensive neuropsychological examination. The degree of dementia, as evaluated by the Mini-Mental State Examination (MMSE), varied from mild to very mild, ranging from 18 to 29. Eleven of the AD patients had been on cholinesterase inhibitor treatment for 2 to 4 years (five rivastigmine and six galantamine). Five recently diagnosed AD patients had never received treatment before the study. There was no significant

difference in age or education level between the AD patients and the OC subjects (see Table 2).

All AD patients and their next of kin and all HC subjects gave informed consent to participate in the study. The study was approved by the Ethics Committee of Uppsala University and Karolinska Institute, Stockholm, the Isotope Committee, Uppsala University Hospital, Uppsala, Sweden, and the Institutional Review Board of the University of Pittsburgh.

Positron Emission Tomography

Patients and healthy volunteers were examined after fasting for at least 6 hours before PET. Electrocardiography, pulse and blood pressure were measured throughout the PIB study. PET was performed in either of two Siemens ECAT HR+ cameras with an axial field of view of 155mm, providing 63 contiguous 2.46mm slices with a 5.6mm transaxial and a 5.4mm axial resolution. The orbitomeatal line was used to center the head of the subjects. The data were acquired in three-dimensional mode. The patients and healthy volunteers were given an intravenous injection of approximately 300MBq of PIB. PET measured the time-dependent uptake of radioactivity in the brain according to a predetermined set of measurements (frames 2×60, 3×120, 4×180, 4×300, and 2×600 seconds) for 1 hour.

Subjects were given 200 to 300MBq of ^{18}FDG intravenously and PET measured the radioactivity in the brain for 5×60, 5×180, 5×300, and 1×600 seconds frames for 55 minutes. The plasma glucose concentration was measured three times, once before and twice after the ^{18}FDG injection. All ^{18}FDG scans of AD patients were obtained within 30 days of the PIB scan.

Attenuation correction was based on a 10-minute windowed transmission scan with rotating ^{68}Ge rod sources before administration of the radioactivity. The emission data were normalized, corrected for random coincidences and dead time, and corrected for scatter using a method by Watson and colleagues.[15] Images were reconstructed with the standard software supplied with the scanner (ECAT 7.1; CTI PET Systems, Knoxville, TN), using Fourier rebinning followed by two-dimensional filtered back-projection applying a 4mm Hanning filter. A computerized reorientation procedure was used to align consecutive PET studies for accurate intra- and interindividual comparisons.[16]

Metabolite Analysis

Arterialized-venous blood samples were obtained from 13 AD patients and 4 OC subjects. Radial artery blood samples were obtained in 2 of the 3 YC subjects, 2 of the 6 OC subjects, and 3 of the 16 AD patients (AD12, AD13, and AD14). Whole-blood samples were centrifuged and an equal volume of acetonitrile was added to the plasma fraction to precipitate the proteins. The supernatant was analyzed by high-performance liquid chromatography. Separation of metabolites and tracer was performed on a Genesis C18 column with a mobile phase consisting of acetonitrile 50mM ammonium formate, pH 3.5 (55:45, vol/vol). The metabolite and tracer fractions were collected and the radioactivity was measured in a well-type scintillation counter.

Regions of Interest

All PET investigations were analyzed using identical standardized regions of interest (ROI) in the brain.[17] Cortical ROI (1×3cm) were placed in the frontal (three slices) and parietal (four slices) cortices. ROI for the striatum were placed at the level with highest uptake. Other cortical ROI were placed in the occipital and cerebellar cortices at the level of highest radioactivity uptake and in the temporal cortices (five coronal slices). Two ROI (1.5cm in diameter) were located in the pons and linked, and the subcortical white matter was defined with a traced ROI at the location of centrum semiovale. The parietal, temporal, frontal, and occipital ROI were linked to form volumes of interest.

Image Quantitation

Arterial plasma data were available for 7 of the 25 subjects, but 2 of the AD patients were among the 3 outliers that did not show PIB retention (see below). Therefore, arterial data were available for only one subject who showed significant PIB accumulation (AD13). This precluded conventional compartmental analysis on the subject group as a whole. Reference tissue modeling using the cerebellum then was explored. The cerebellum was chosen as a reference region because of its previously reported lack of Congo red and thioflavin-S–positive plaques.[18,19] Over the 60-minute time frame that the data were collected, the tissue-to-reference ratio did not plateau over a sufficient number of points to validly apply steady state–based modeling methods (eg, Logan graphical analysis[20,21]). Future studies with extended periods of data acquisition of at least 90 minutes should allow for definitive determination of whether or not steady state–based methods can be applied. Models which assume irreversible binding (eg, Gjedde[22] and Patlak and colleagues[23,24]) also were applied to the data, but difficulties were observed in brain areas with very low accumulation, such as the cortical regions of HC subjects. There was some indication that this may be caused by a small but significant net accumulation of tracer in the cerebellum, perhaps because of nonspecific retention in the white matter which contaminates this reference ROI. Efforts are under way to analyze the data with a modified Patlak method that corrects for this accumulation in the reference region. The details of this analysis will be presented separately elsewhere (G. Blomqvist, in preparation). Currently, expressing the data in terms of standardized uptake value (SUV) appears preferable because it does not introduce assumptions about the kinetics which have not yet been adequately explored. SUV was obtained by normalizing tissue concentration (nCi/ml) by injected dose (nCi) and body mass (in units of ml, making the approximation that 1gm equals 1ml). Note that, although not yet optimized, preliminary modeling approaches produced results that were entirely consistent with the SUV results.

^{18}F-fluorodeoxyglucose Analysis

Parametric maps of glucose metabolic rate ($rCMR_{glc}$) were generated by the Patlak technique using the time course of the tracer in arterialized-venous plasma as the input function.[22,23] Taking advantage of the 20-minute half-life of carbon 11, ^{18}FDG scans could be performed 120 minutes after the injection of PIB.

Statstical Analyses

Statistical comparisons utilized a two-sample, unequal variance, two-tailed Student's t test. Linear regression analyses were conducted to yield the Pearson product moment correlation coefficient, r. Because of the multiple comparisons in eight brain areas, a Bonferroni correction was applied to set statistical significance to p value of 0.05/8 (ie, $p = 0.006$) to declare a significant difference to be present between two groups.

Results

Characterization of PIB Binding to Postmortem Tissue

In sections of fresh-frozen postmortem tissue, PIB showed little binding to the amyloid-free frontal cortex of a cognitively normal elderly control brain (Fig 2A, B). In contrast, PIB bound specifically to the amyloid-laden frontal cortex of an age-matched AD brain in a manner that could be blocked by an excess of the structural analog, BTA-1 (see Fig 2C, D). The nonspecific retention of PIB in white matter was overshadowed by the cortical binding in AD brain but predominated in control brain (see Fig 2). Note that Figure 2 represents fresh-frozen tissue sections that have not been treated to mask white matter binding (ie, the tissue was not defatted and washings were performed using phosphate-buffered saline without ethanol).

Plasma Metabolism of PIB

The plasma concentration of PIB was studied in the nine HC subjects and 16 AD patients. All PIB metabolites were very polar. No substantial differences in the metabolism of PIB were seen between the AD patients and the HC subjects. The amount of unchanged PIB decreased rapidly and was 65.5 ± 8.7% in HC subjects and 68.1 ± 12.9% in AD patients after 5 minutes, 30.7 ± 7.3% (HC) and 33.5 ± 8.9% (AD) after 12 minutes, and 7.2 ± 3.6% (HC) and 9.8 ± 3.0% (AD) after 60 minutes. Furthermore, no differences between the time course of labeled metabolites in arterial and/or venous plasma could be seen. Of note, in vivo mouse studies using PIB showed similarly rapid peripheral metabolism, whereas greater than 95% of the radioactivity in brain could be recovered as unchanged parent compound.[10] Studies in other species are ongoing.

Time-Activity Data

The six OC subjects showed a brain entry and clearance pattern very similar to that found in the YC subjects, and there was no statistically significant difference between the two healthy control (HC) groups. Therefore, young and older control groups were combined to form the HC group for comparison with the AD patients. All statistically significant findings reported below remained significant ($p < 0.006$) in a separate analysis comparing AD patients to only the six OC subjects. The data from 1 of the 16 AD patients (AD1) were excluded from the SUV analyses because of low radioactivity values in all brain areas (including cerebellum and white matter), possibly caused by extravasation of an unknown portion of the injected dose.

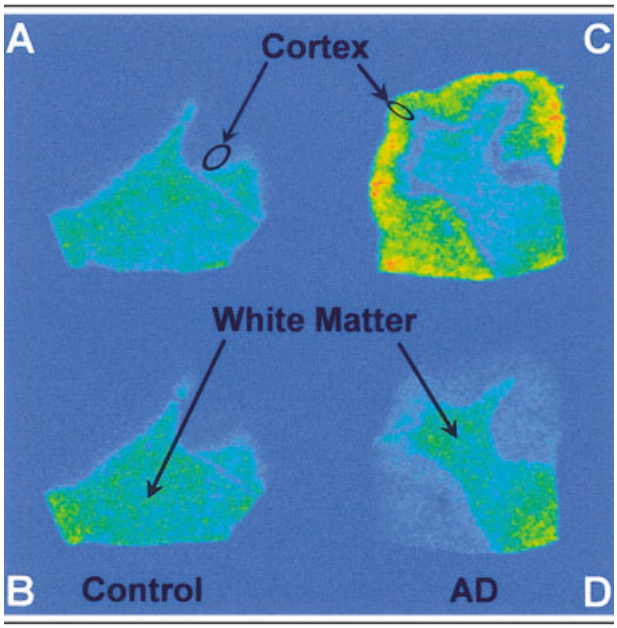

Fig 2. Specific and displaceable PIB binding occurs in the cortex of postmortem Alzheimer's disease (AD) brain, but not in white matter or control brain cortex. Autoradiograms showing the binding of PIB to fresh-frozen, post-mortem control (A, B) and AD brain sections (C, D). All sections were incubated with 10nM PIB. Excess nonradioactive BTA-1(10μM) was added in B and D to demonstrate displaceable binding. Arrows indicate the location of white matter and cortex (gray matter area is circled in A, C). Cortex is barely visible on control sections because of lack of binding.

As a group, the HC subjects showed rapid entry and clearance of PIB in all cortical and subcortical gray matter areas, including cerebellar cortex (Fig 3A, C, D). Cerebellum, an area lacking fibrillar amyloid plaques, showed nearly identical uptake and clearance of PIB in the HC and AD groups (see Fig 3A). Subcortical white matter showed relatively lower entry and slower clearance in both HC subjects and AD patients, but PIB retention did not differ significantly between the two groups (see Fig 3B). In contrast, the AD patients showed a marked retention of PIB compared with HC subjects in areas of the brain known to contain large amounts of amyloid deposits in AD, such as parietal and frontal cortices[25,26] (see Fig 3C, D, E). The SUV values over the late time points (40–60 minutes) were averaged to calculate the SUV values shown in the group comparisons and to generate the images shown below.

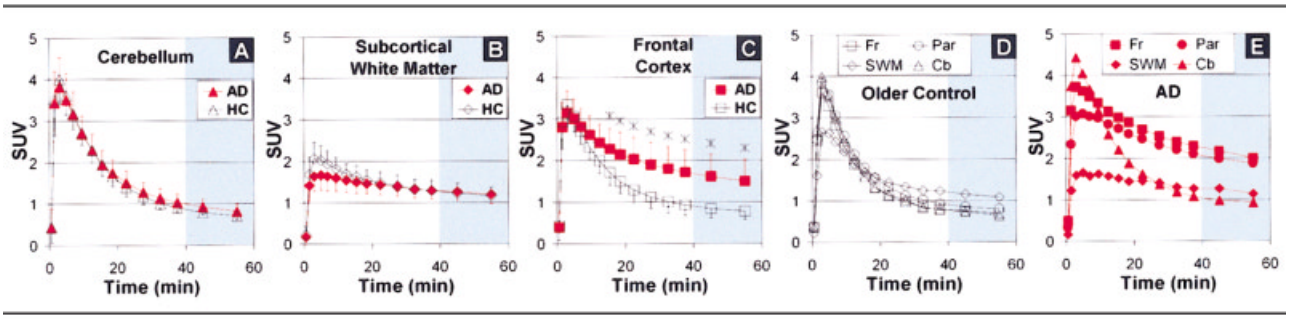

*Fig 3. PIB is differentially retained only in amyloid-laden cortical areas of AD brain. Standardized uptake values (SUVs) demonstrating brain entry and clearance of PIB. A to C represent averaged SUV values for all HC subjects (*open, black symbols*; n = 9) and all AD patients (*filled, red symbols*; n = 15) in cerebellum, subcortical white matter, and frontal cortex. D and E show brain entry and clearance in cerebellum* (triangles)*, subcortical white matter* (diamonds)*, frontal cortex* (squares)*, and parietal cortex* (circles) *for an older control subject (D) and an AD patient (E). Error bars represent one standard deviation (SD) and are too small to be seen in some of the HC subject data in A to C. Asterisks (e.g., in C) indicate a significant difference between AD and HC values (*$p < 0.006$*). Shaded areas highlight the 40 to 60-minute time period used for the summed SUV data displayed in Figures 4 to 7.*

Standardized Uptake Value Images

As the time-activity data would predict, the topographical pattern of PIB retention was clearly different in AD patients compared with the HC subjects (Fig 4). PIB accumulation in AD patients as a group was most prominent in cortical association areas and lower in white matter areas. This pattern is very consistent with that described in postmortem studies of amyloid deposition in AD brain.[25,26] PIB images from HC subjects showed little or no PIB retention in cortical areas, leaving the subcortical white matter regions highest in relative terms. Note that, in absolute terms, the accumulation of PIB in white matter was essentially the same in AD patients and HC subjects (see Figs 3B, 6B).

A series of axial and sagittal images give a better three-dimensional sense of the topography of PIB retention (Fig 5). The marked difference between PIB retention in the AD patient and the HC subject is apparent throughout most of the forebrain. Frontal cortex was widely affected in the AD patient, but intense PIB retention also was observed in temporal and parietal cortices, portions of occipital cortex, and in the striatum. Lateral temporal cortex appeared to have greater PIB accumulation than medial temporal areas. Cerebellar cortex (see Fig 5) showed little PIB retention and was similar in AD patients and HC subjects.

Quantitative Comparisons of Alzheimer's Disease and Healthy Control Group Data

In cortical areas, the mean PIB SUV value of AD patients was significantly greater than the mean PIB SUV value of control subjects (Fig 6A; Table 3). This indicates increased retention of PIB in areas known to have extensive amyloid deposition in AD.

Three patients diagnosed with AD (AD4, AD12, and AD14) had high MMSE scores (28–29) and

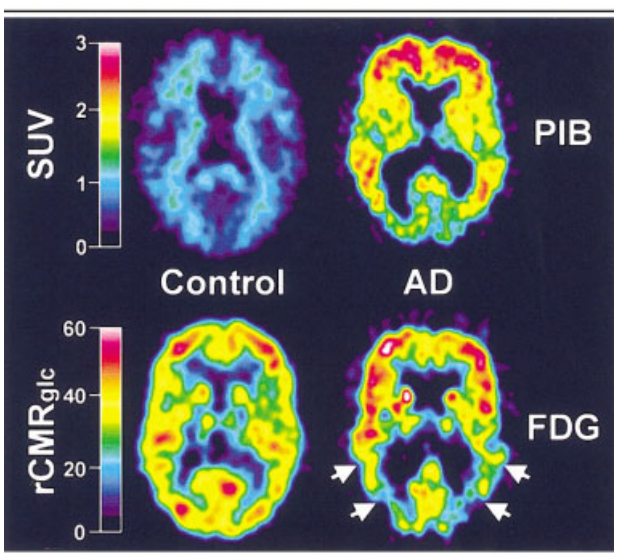

Fig 4. PIB standardized uptake value (SUV) images demonstrate a marked difference between PIB retention in Alzheimer's disease (AD) patients and healthy control (HC) subjects. PET images of a 67-year-old HC subject (left) and a 79-year-old AD patient (AD6; MMSE = 21; right). (top) *SUV PIB images summed over 40 to 60 minutes;* (bottom) ^{18}*FDG* $rCMR_{glc}$ *images (μmol/min/100ml). The left column shows lack of PIB retention in the entire gray matter of the HC subject (top left) and normal* ^{18}*FDG uptake (bottom left). Nonspecific PIB retention is seen in the white matter (top left). The right column shows high PIB retention in the frontal and temporoparietal cortices of the AD patient (top right) and a typical pattern of* ^{18}*FDG hypometabolism present in the temporoparietal cortex (*arrows*; bottom right) along with preserved metabolic rate in the frontal cortex. PIB and* ^{18}*FDG scans were obtained within 3 days of each other.*

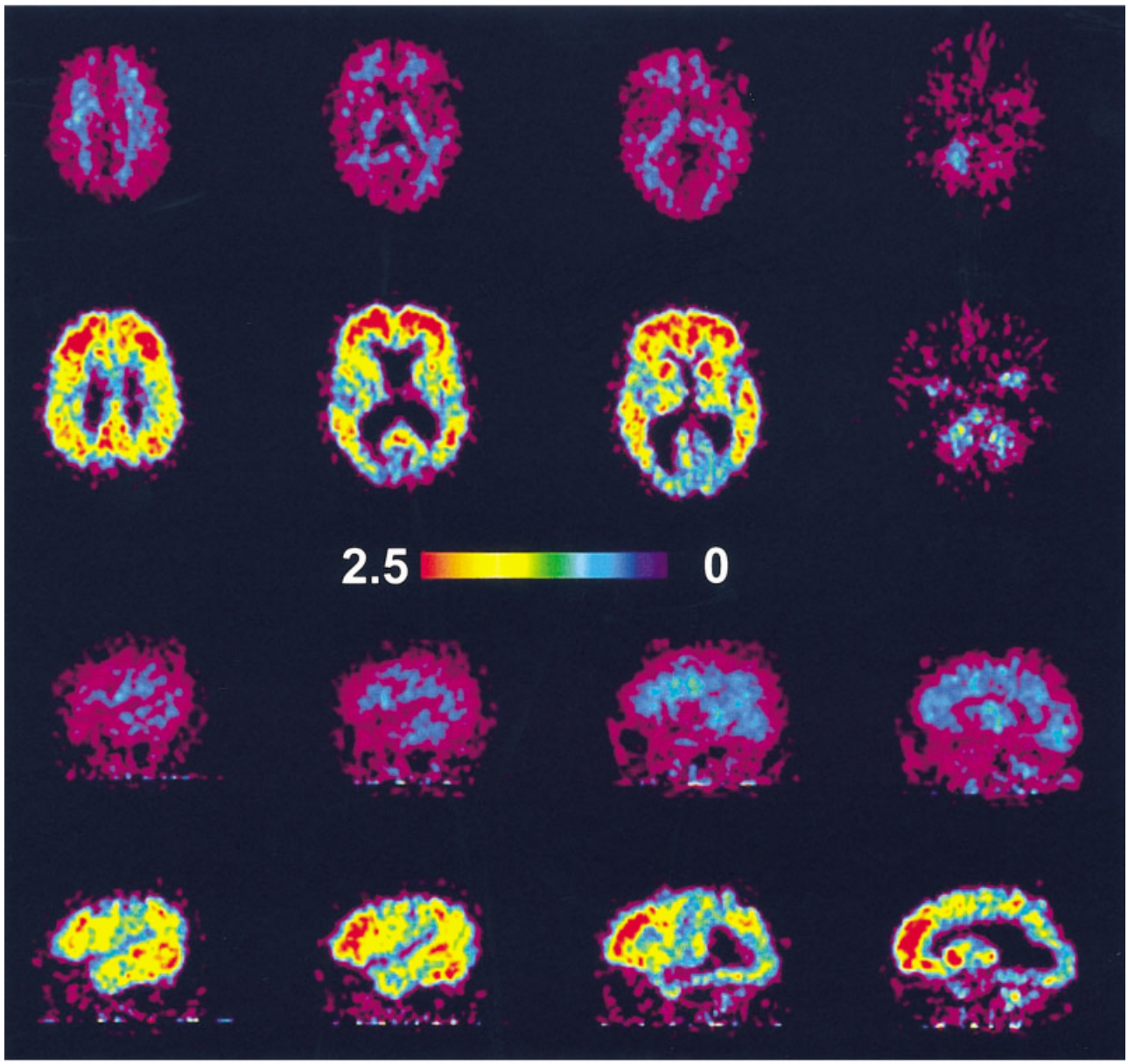

Fig 5. Serial planes demonstrate the topography of PIB retention. Axial (top two rows) and sagittal (bottom two rows) standardized uptake value (SUV) PIB images of the subjects shown in Figure 4. The healthy control subject data are shown in rows 1 and 3. The Alzheimer's disease patient data are shown in rows 2 and 4. The reference region, the cerebellum, can best be appreciated in the images at the far right. The cerebellar peduncles (white matter) show some nonspecific retention, but the cerebellar cortex shows negligible retention. Scale bar indicates relative levels of PIB SUV values.

showed no significant deterioration over the 2 to 4-year follow-up period (see Table 1). These subjects had levels of PIB retention in cortical regions typical of controls (see open triangles in Fig 6). They also had $rCMR_{glc}$ values similar to controls in the brain areas presented in Figure 6. These three subjects were retained in the AD group for all analyses. In the OC group, the oldest subject consistently showed the highest cortical PIB retention and the lowest cortical $rCMR_{glc}$ (see boxed circles in Fig 6). This subject had not expressed any subjective memory complaints and performed within the reference range on the neuropsychological test battery except for difficulty copying a complex cube.

The average PIB SUV values in the HC subjects were low and similar to each other in all cortical and

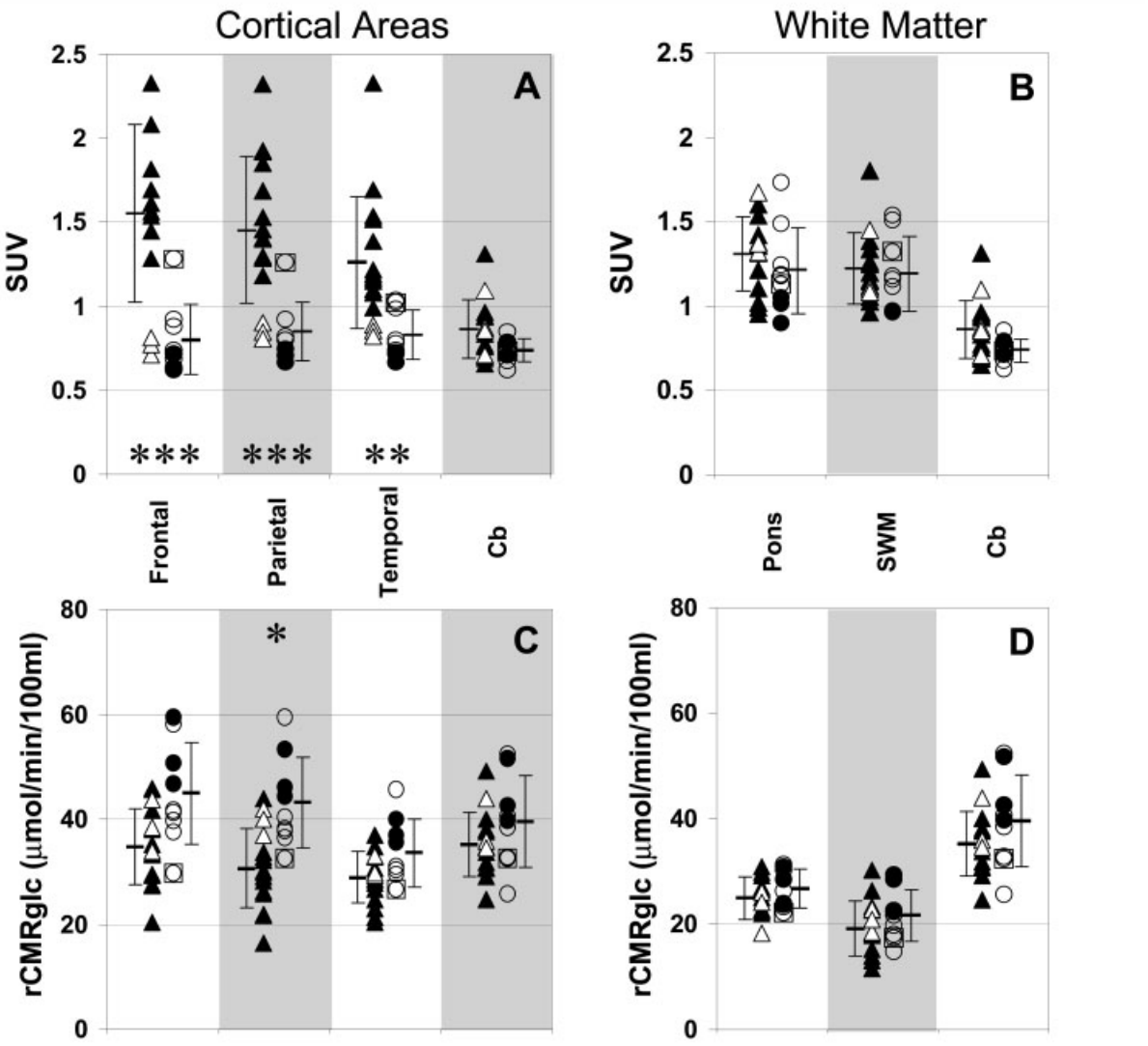

Fig 6. The differences in PIB retention between Alzheimer's disease (AD) patients and healthy control (HC) subjects can be quantified and are statistically significant. Shown is the accumulation of PIB and rCMRglc in selected regions. Average PIB standardized uptake value (SUV) values were summed over 40 to 60 minutes in cortical areas (A) or white matter areas (B) and compared with cerebellum. Values for ^{18}FDG uptake were calculated with the Gjedde-Patlak method in cortical areas (C) or white matter areas (D) and compared with cerebellum. The mean and one SD are indicated with the error bars beside the individual points. HC subjects: circles*; n = 9;* filled circles *represent the three young HC subjects;* boxed circle *represents the outlier in the HC group (oldest subject). AD patients:* triangles*; n = 15 (SUV) or n = 16 (FDG);* open triangles *represent the three outliers in the AD group. AD mean and SD values include all 15 (SUV) or 16 (^{18}FDG) AD subjects;* $p < 0.01$ *(*);* $p < 0.002$ *(**);* $p < 0.0002$ *(***).*

subcortical gray matter areas. In HC subjects and AD patients, the retention also was similar in the cerebellar gray matter (see Table 3), a cortical area that lacks fibrillar amyloid plaques.[18] This indicates the lack of PIB retention in control cortex and in the cerebellum of both AD and controls, brain areas which would not be expected to have significant amyloid deposition.

In HC subjects, the PIB SUV values in pons and subcortical white matter (see Fig 6B) were higher than in cortical areas and very similar to the SUV values found in pons and subcortical white matter of AD patients (see Table 3). This suggests higher, nonspecific retention of PIB in white matter than in gray matter areas.

We found the striatum, consistent with previous reports of extensive amyloid deposition in the striatum of virtually all AD patients,[27–30] to have significantly higher PIB retention in AD patients than in HC subjects (see Table 3).

Table 3. PIB Retention in Various Brain Areas (SUV)

	Fr	Par	Temp	Occ	Striatum	Pons	SWM	Cb
AD mean (n = 15)	1.56	1.45	1.26	1.24	1.47	1.31	1.22	0.86
AD SD	0.53	0.43	0.39	0.43	0.41	0.22	0.21	0.17
HC mean (n = 9)	0.80	0.85	0.83	0.80	0.84	1.21	1.19	0.74
HC SD	0.21	0.18	0.15	0.13	0.19	0.26	0.22	0.07
AD vs HC (p)	**0.0001**	**0.0001**	**0.0011**	**0.0017**	**0.00004**	0.3563	0.7238	0.0205
AD:HC ratio	1.94	1.71	1.52	1.54	1.76	1.08	1.03	1.17

Statistically significant results ($p < 0.006$) are boldface and underlined.

SUV = standardized uptake value; AD = Alzheimer's disease; HC = healthy control; SD = standard deviation.

Comparison of PIB Retention to Cerebral Metabolic Rate

The $rCMR_{glc}$ in cortical areas was lower in the AD patients compared with HC subjects in most regions (Table 4) as has been established in many previous studies.[31–34] The largest and only significant difference ($p < 0.006$) in $rCMR_{glc}$ was observed in parietal cortex (see Fig 6C; Table 4). The relative differences in $rCMR_{glc}$ between AD patients and HC subjects were in general smaller (eg, 41% in parietal cortex; see Table 4) than the relative differences in PIB retention (eg, 94% in frontal cortex; see Table 3). The correlation between PIB retention and $rCMR_{glc}$ in all subjects and in AD patients alone is shown in Table 4. When all HC subjects and AD patients were combined, a significant negative correlation ($p < 0.006$) was observed only in the parietal cortex (Fig 7). Clear negative trends were observed in all cortical areas, but not in white matter areas. These correlations did not remain significant at the p value 0.006 level (see Subjects and Methods) when only AD patients were included, although the negative trend remained obvious in the parietal cortex (see Table 4, Fig 7).

The relative changes in PIB and $rCMR_{glc}$ for each individual patient also can be appreciated from the data in Figure 7. For this purpose, low $rCMR_{glc}$ values were defined as those more than one SD below the mean $rCMR_{glc}$ of the HC subjects (ie, $rCMR_{glc}$ $<34.6\mu$mol/min/100ml) and high PIB SUV values were defined as those more than one SD above the mean PIB SUV of the HC subjects (ie, PIB SUV >1.03). These areas are indicated in Figure 7, and it can be seen that all AD patients with abnormally low parietal rCMRglc values also had abnormally high parietal PIB SUV values. Interestingly, all three AD patients (MMSE 28–29) with parietal PIB SUV values less than 1.03 also had normal parietal rCMRglc values (see open triangles in Fig 7). However, one AD patient with a normal rCMRglc had a high PIB SUV value (see double asterisks in Fig 7). None of the HC subjects with PIB SUV values less than 1.03 showed low rCMRglc values. The one HC subject (the

Table 4. rCMRglc and Correlation to PIB Retention

	Fr	Par	Temp	Occ	Striatum	Pons	SWM	Cb
rCMRglc (μmol/min/100 ml)								
AD mean (n = 16)	34.8	30.6	28.9	38.5	47.8	25.2	19.0	34.9
AD SD	7.2	7.6	4.9	6.6	6.8	3.9	5.1	6.0
HC mean (n = 9)	45.0	43.2	33.6	49.3	55.5	26.7	21.6	39.6
HC SD	9.7	8.6	6.4	10.3	11.4	3.6	4.9	8.7
(AD vs HC) (p)	0.0163	**0.0024**	0.0801	0.0149	0.0914	0.3304	0.2255	0.1716
AD:HC ratio	0.77	0.71	0.86	0.78	0.86	0.94	0.88	0.88
Correlation of rCMRglc to PIB SUV								
All Subjects (n = 24)								
r	−0.43	−0.72	−0.31	−0.48	−0.26	0.28	−0.08	−0.19
p	0.037	**0.0001**	0.187	0.017	0.323	0.266	0.99	0.776
AD only (n = 15)								
r	−0.03	−0.61	−0.15	−0.34	−0.03	0.34	0.27	−0.32
p	0.99	0.015	0.99	0.258	0.99	0.257	0.438	0.305

Statistically significant results ($p < 0.006$) are boldface and underlined.

rCMRglc = regional cerebral glucose metabolic rate; AD = Alzheimer's disease; SD = standard deviation; HC = healthy control; SUV = standardized uptake value.

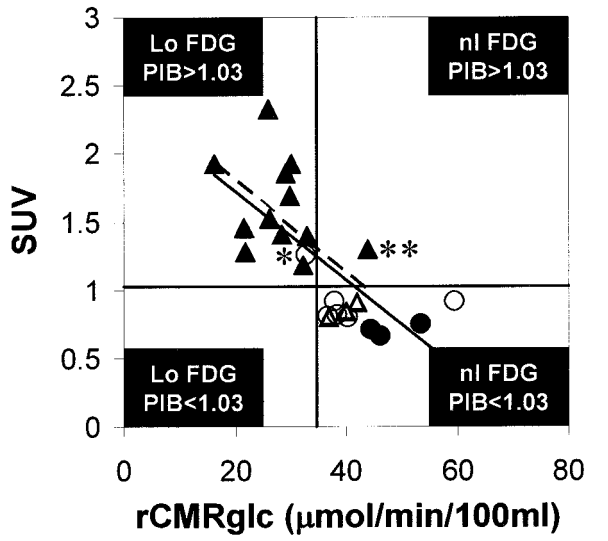

Fig 7. PIB retention is inversely correlated with $rCMR_{glc}$. Correlation of $rCMR_{glc}$ in parietal cortex versus parietal PIB standardized uptake value (SUV) values. Correlations were performed separately on all subjects (n = 24, R^2 *= 0.511;* p *= 0.0001;* solid line*) and only Alzheimer's disease (AD) patients (n = 15,* R^2 *= 0.377;* p *= 0.015;* dotted line*). AD patients are represented by* triangles *(outliers are* open triangles*) and HC subjects are represented by* circles *(young controls are* filled circles*). Also indicated is a horizontal line that represents one SD above the HC mean PIB SUV value (at 1.03 SUV) and a vertical line that represents one SD below the HC mean rCMRglc (at 34.6μmol/min/100ml). See text for further details.*

oldest) with a slightly low rCMRglc value also had an increased PIB SUV value (see single asterisk in Fig 7).

Correlations between PIB Retention and Clinical/ Biochemical Variables

There was a trend in all brain areas for higher PIB SUV values to be observed in AD patients having lower MMSE scores, but none of these correlations reached statistical significance. There was no significant correlation of PIB retention with age in either the AD or HC groups. However, the oldest HC subject showed consistently higher PIB retention than the other controls (see Fig 6).

In the AD patient group, there was no significant correlation in any brain area studied between PIB SUV values and duration of illness (from either onset or time of diagnosis) or number of years on cholinesterase inhibitors. Comparing AD patient subtypes, treatment with cholinesterase inhibitors and sex showed no significant effect on PIB values in any brain area. ApoE genotype had no effect on PIB SUV values in any brain area of AD patients. Furthermore, there was no trend toward increased PIB SUV values in the 4/4 AD patients (n = 6) compared with the 3/3 AD patients (n = 8).

Discussion

In autoradiographic studies of postmortem brain tissue, PIB showed specific and displaceable binding to AD cortical areas containing amyloid deposits, but not to control cortex. These studies are consistent with several previous studies which support the specificity of benzothiazole, thioflavin-T derivatives for amyloid deposits.[8,10–12] Plasma metabolism of PIB was rapid and all metabolites were polar, suggesting that blood metabolites are not likely to enter the brain. This is consistent with metabolic data in mice.[10] Further studies are under way in other species and with human tissue in vitro to determine whether radioactive metabolites could be present in human brain. Determination of the optimal pharmacokinetic modeling method will be ongoing as more arterial data are collected and scan time is increased to 90 minutes. Until this issue can be clarified, we prefer to express the data in terms of SUV.

In this study, both imaging and time-activity curves showed that the retention of PIB provided a quantifiable discrimination between most mild AD patients and HC subjects. In HC subjects, there was very little retention of PIB in cortical regions. In contrast, frontal and temporoparietal cortical areas, known to contain amyloid deposits in AD, showed preferential retention of PIB. The absolute level of PIB retention was approximately the same in the cerebellum and white matter of AD patients and HC subjects, brain areas known to lack substantial deposits of fibrillar amyloid. Time-activity curves demonstrated that the absolute amount of PIB retained in the frontal cortex of AD patients was greater than 90% higher than that retained in control frontal cortex or cerebellum of either controls or AD patients.

In general, this pattern of PIB retention is consistent with the pattern of amyloid plaque deposition described in postmortem studies of AD brain.[25,26] These postmortem studies showed that, from the earliest stages, amyloid plaque deposition was distributed fairly evenly across neocortical association cortices in AD. In contrast, mesial temporal lobe areas (including hippocampus) showed relatively low plaque burdens.[26] Unlike plaque deposition, the topographical development of neurofibrillary tangles begins focally in the transentorhinal cortex and progresses predictably through limbic areas to the neocortex.[35] PIB retention typically predominated in frontal cortex, but note that frontal cortex did not always show the highest PIB retention in a given subject and mean levels of frontal PIB retention exceed parietal levels by less than 10%. Postmortem studies using silver stains, antibodies to Aβ, or thioflavin-S do identify frontal cor-

tex as a brain area very high in amyloid deposition but have not identified it as the site of greatest deposition.[25,26] This raises the question of whether the observation of highest PIB retention in the frontal cortex is real or an artefact. There is evidence that the nature of amyloid deposits varies across the neocortex.[36] It also is possible that there are additional regional variations in amyloid processing and fibrillogenesis that can be detected in vivo but cannot be detected in postmortem tissue, particularly after fixation. Another possible reason for the greater PIB SUV values in frontal cortex compared with temporal and parietal cortex could be the fact that, in AD, regional cerebral blood flow (rCBF) to the frontal cortex is relatively preserved compared with the well-described decreases in temporal and parietal cortex.[37] Currently, the presence or absence of a rCBF effect on PIB measures has not yet been determined, and careful studies exploring the relationship between changes in rCBF and PIB retention will be needed to fully address this issue. Whether or not SUV measures of PIB retention are found to be affected by rCBF differences, compartment models will be applied to PIB data in the future and the optimal PIB retention measures derived from these models would be expected to be much less influenced by rCBF differences than those derived from SUV-type analyses.

Extensive amyloid deposition has been reported to occur in the striatum of virtually all AD patients,[28–30] and we observed substantial PIB retention in the striatum of AD patients in this study. Striatal plaque deposition appears to occur early in the progression of AD pathology and coincides with neocortical pathology and cognitive changes.[27] Although neuritic elements have been described in ventral striatum,[29] most striatal Aβ deposits are not associated with dystrophic neurites.[28,29] Despite this poorly understood absence of neuritic changes in the striatum, striatal plaques appear to be fibrillar as evidenced by the fact that they are stained well by the fibril-specific Congo red derivative, X-34.[38] PIB and related benzothiazoles also stain striatal amyloid deposits in postmortem AD brain (W.E. Klunk, unpublished data) in a manner similar to the staining of cortical deposits by other benzothiazole derivatives.[11] Therefore, the observation of significant PIB retention in the striatum is not surprising.

Three patients with very mild AD (AD4, AD12, and AD14) had cortical PIB retention similar to the HC subjects. Note that these three patients had MMSE scores between 28 and 29 after 2 to 4 years of follow-up. At the time of the PIB study, AD4, AD12, and AD14 all had temporal and parietal rCMRglc values that were not typical of AD patients and more closely resembled the HC subjects. Other mild AD patients with similar clinical profiles showed typical AD-like changes in PIB retention and $rCMR_{glc}$. For example AD11, AD13, and AD15 all had an MMSE score of 27 at the time of study but had increased PIB retention and decreased $rCMR_{glc}$. Treatment with cholinesterase inhibitors was not related to the differences observed. Therefore, it is unclear whether this amyloid imaging technique was simply insensitive to the amount of amyloid deposits in the brains of AD4, AD12, and AD14 or whether PIB imaging has correctly identified subjects without amyloid deposits in whom the clinical diagnosis would not be confirmed by postmortem evaluation.

Conversely, the oldest control in this study showed PIB retention typical of AD patients and could be described as an asymptomatic amyloid-positive case. This type of case brings up issues of specificity versus early detection. One possibility could be that a high PIB signal was obtained in the absence of amyloid deposits (ie, a false-positive). However, if this finding does represent the true presence of amyloid in an asymptomatic individual, the question becomes whether substantial amyloid deposition can be found as part of the normal aging process in subjects who will never develop AD[39] or is increased amyloid deposition always a sign of preclinical AD[40–42]? The ability to longitudinally follow PIB retention as an in vivo measure of amyloid deposition now gives us a tool through which we may be able to answer this question in a manner that postmortem studies can not.

Note that this initial proof-of-concept study was not designed to determine the sensitivity and specificity of amyloid imaging with PIB for the diagnosis of AD. Many very mild cases (MMSE $\geq$25 in 12 of 16 cases) were included, and the accuracy of the clinical diagnosis of AD is not clearly defined at this stage. Therefore, we cannot assess the utility of PIB for the diagnosis of AD from this study. Further studies that include only more typical, moderately impaired AD patients will be needed to address sensitivity issues and more controls and patients with non-AD dementias must be studied to define specificity issues.

The coupling between increased PIB retention and decreased ^{18}FDG metabolism was not an unexpected finding, given the well-known decrease in temporoparietal metabolism in AD patients[31] and the presence of extensive amyloid deposition in these same areas.[25,26] PET with ^{18}FDG and PIB might be considered as complementary methods, one looking directly at amyloid pathology and the other looking at metabolic dysfunction at the synapse that may or may not be related to the local pathology. Thus far, we have studied only mild AD patients with PIB, but ^{18}FDG imaging has been shown to be sensitive enough to demonstrate metabolic changes before the onset of clinical symptoms in subjects at risk for AD due to the presence of the ApoE4 allele[43,44] or the presence of chromosome

21 or 14 mutations.[45,46] Inevitably, a comparison of the relative "sensitivities" of imaging with PIB and ^{18}FDG for detecting changes in the brains of AD patients will be necessitated. Our data showed that the largest mean difference between AD patients and HC subjects in $rCMR_{glc}$ was approximately 40% in the parietal cortex (or approximately 1.5 SD from the control mean), whereas the largest mean difference in PIB retention was greater than 90% in frontal cortex (or approximately 3.6 SD from the control mean). All AD patients with low parietal $rCMR_{glc}$ also had high PIB retention, but one AD subject (AD16) with normal parietal $rCMR_{glc}$ had elevated PIB retention.

No significant correlation was observed between PIB accumulation and MMSE scores in this sample of AD patients, but this may be because 12 of the 16 AD patients fell into the narrow range of 25 to 29 on MMSE score. In this initial study, the reported association between ApoE4 genotype and increased postmortem cortical amyloid load was not reflected by increased PIB retention in AD patients having an ApoE4 allele.[47,48] However, the relationship between ApoE4 and postmortem amyloid load is complex and not always observed.[49]

Although this "proof-of-concept" study represents the first evaluation of a benzothiazole compound as an in vivo radiotracer for imaging amyloid deposition in human brain, two previous attempts have been made to image amyloid deposition in living AD patients using other tracers. The first attempt used single-photon emission computed tomography and a ^{99m}Tc-labeled antibody to Aβ, but there was no evidence of cerebral uptake of the antibody.[50] The second in vivo human amyloid-imaging study used the tracer ^{18}F-FDDNP to quantify amyloid in nine AD patients and seven controls.[51] The time-activity data from an AD patient included in that study indicated that, at late time points (90–120 minutes), the absolute retention of ^{18}F-FDDNP in neocortical areas exceeded that in the reference region, the pons, by 10 to 15%. The area of highest retention at late time points was the hippocampus/amygdala/entorhinal cortex region, an area that exceeded the reference region by approximately 30%.

As the technology of amyloid imaging moves forward, it will be important to avoid the circular reasoning inherent in the association of amyloid deposition with both the diagnosis and the cause of AD. Therefore, at the outset, it may be best to not equate amyloid deposition to clinical diagnosis. Rather than as a method of diagnosis, it might be best to first think of PIB retention more fundamentally as a method to detect and quantify brain β-amyloidosis, a term first used in reference to AD by Glenner.[52] Several basic, unbiased questions then can be asked regarding (1) the correlation of β-amyloidosis with clinical diagnosis; (2) the natural history of β-amyloidosis and its onset relative to clinical symptoms of dementia; and (3) the ability of β-amyloidosis to serve as a surrogate marker of efficacy for antiamyloid therapeutics.

The relationship of brain β-amyloidosis to clinical AD and the natural history of that relationship can be determined only by large and careful longitudinal human studies. We have so far investigated only mild AD patients. To sort out the relationship between brain β-amyloidosis and AD, it will be important to perform further studies in subjects with mild cognitive impairment, carriers of familial AD mutations and other types of increased genetic risk, and in larger groups of AD patients and HC subjects. Another potential use of in vivo amyloid imaging could be as an aid to the development of a variety of antiamyloid therapeutic candidates. Such antiamyloid drug studies may provide new knowledge concerning the relevance of β-amyloidosis to the clinical symptoms of AD. Although these and other issues are yet to be fully resolved, this study strongly suggests that PIB retention may be a good indicator of amyloid deposition in vivo.

This work was supported by grants from the Alzheimer's Association (IIRG-95-076, TLL-01-3381, W.K.; NIRG-00-2335, Y.W.), the NIH (National Institute of Aging), AG01039, AG20226, W.K.; AG18402 C.M.), Institute for the Study of Aging/American Federation for Aging Research (Y.W.), the Swedish Medical Research Council (project 05817, A.N.), and the Stohnes Foundation (A.N.).

Brain tissue for autoradiography was provided through the University of Pittsburgh Alzheimer Disease Research Center Brain Bank (AG05133) by Drs S. T. DeKosky and R. L. Hamilton. We thank R. Öhrstedt, L. Lindsjö, M. Lidholm, A. Pettersson, and G. Nylén for their role in performing the PET examinations.

Disclosure

During the process of this study, Amersham Health provided research grant support to the University of Pittsburgh and entered into a License Agreement with the University of Pittsburgh based on the technology described in this article. Drs Klunk, Mathis, and Wang are coinventors of PIB and, as such, have a financial interest in this License Agreement. Also during the process of this study, the Uppsala University PET Centre became partially owned by a subsidiary of Amersham Health called Imanet and was named Uppsala Imanet AB. Uppsala Imanet AB is a joint venture created by Amersham Health and Uppsala University Holdings. All authors listed as having a Uppsala Imanet AB affiliation are Imanet employees. Dr Langstrom holds the titles of Head of R&D of Uppsala Imanet AB and Chief Scientific Officer of Imanet.

References

1. Klunk WE, Debnath ML, Pettegrew JW. Development of small molecule probes for the beta-amyloid protein of Alzheimer's disease. Neurobiol Aging 1994;15:691–698.

2. Zhen W, Han H, Anguiano M, et al. Synthesis and amyloid binding properties of rhenium complexes: preliminary progress toward a reagent for SPECT imaging of Alzheimer's disease brain. J Med Chem 1999;42:2805–2815.
3. Dezutter NA, Dom RJ, de Groot TJ, et al. 99mTc-MAMA-chrysamine G, a probe for beta-amyloid protein of Alzheimer's disease. Eur J Nucl Med 1999;26:1392–1399.
4. Wengenack TM, Curran GL, Poduslo JF. Targeting Alzheimer amyloid plaques in vivo. Nat Biotechnol 2000;18:868–872.
5. Klunk WE, Wang Y, Huang G-F, et al. Uncharged thioflavin-T derivatives bind to amyloid-beta protein with high affinity and readily enter the brain. Life Sci 2001;69: 1471–1484.
6. Agdeppa ED, Kepe V, Liu J, et al. Binding characteristics of radiofluorinated 6-dialkylamino-2- naphthylethylidene derivatives as positron emission tomography imaging probes for beta-amyloid plaques in Alzheimer's disease. J Neurosci 2001;21: RC189.
7. Zhuang ZP, Kung MP, Hou C, et al. Radioiodinated styrylbenzenes and thioflavins as probes for amyloid aggregates. J Med Chem 2001;44:1905–1914.
8. Mathis CA, Bacskai BJ, Kajdasz ST, et al. A lipophilic thioflavin-T derivative for positron emission tomography (PET) imaging of amyloid in brain. Bioorganic Med Chem Lett 2002; 12:295–298.
9. Wang Y, Mathis CA, Huang G-F, et al. Synthesis and evaluation of 2-(3′-iodo-4′-amino)-6-hydroxy-benzothiazole for in vivo quantitation of amyloid deposits in Alzheimer's disease. J Mol Neurosci 2002;19:11–16.
10. Mathis CA, Wang Y, Holt DP, et al. Synthesis and evaluation of ^{11}C-labeled 6-substituted 2-aryl benzothiazoles as amyloid imaging agents. J Med Chem 2003;46:2740–2754.
11. Klunk WE, Wang Y, Huang G-F, et al. The binding of 2-(4′-methylaminophenyl)benzothiazole to post-mortem brain homogenates is dominated by the amyloid component. J Neurosci 2003;23:2086–2092.
12. Bacskai BJ, Hickey GA, Skoch J, et al. Four-dimensional imaging of brain entry, amyloid-binding and clearance of an amyloid-β ligand in transgenic mice using multiphoton microscopy. Proc Natl Acad Sci USA 2003;100:12462–12467.
13. Bergström M, Grahnén A, Långström B. PET-microdosing, a new concept with application in early clinical drug development. Eur J Clin Pharmacol 2003;59:357–366.
14. McKhann G, Drachman D, Folstein M, et al. Clinical diagnosis of Alzheimer's disease: report of the NINCDS-ADRDA work group under the auspices of the Department of Health and Human Services Task Force on Alzheimer's disease. Neurology 1984;34:939–944.
15. Watson CC, Newport D, Casey ME, et al. Evaluation of simulation-based scatter correction for 3D PET cardiac imaging. IEEE Trans Nucl Sci 1997;44:90–97.
16. Andersson JL, Thurfjell L. Implementation and validation of a fully automatic system for intra- and interindividual registration of PET brain scans. J Comput Assist Tomogr 1997;21: 136–144.
17. Engler H, Lundberg PO, Ekbom K, et al. Multitracer study with positron emission tomography in Creutzfeldt-Jakob disease. Eur J Nucl Med Mol Imaging 2003;30:85–95.
18. Joachim CL, Morris JH, Selkoe DJ. Diffuse senile plaques occur commonly in the cerebellum in Alzheimer's disease. Am J Pathol 1989;135:309–319.
19. Yamaguchi H, Hirai S, Morimatsu M, et al. Diffuse type of senile plaques in the cerebellum of Alzheimer- type dementia demonstrated by beta protein immunostain. Acta Neuropathol 1989;77:314–319.
20. Logan J, Fowler JS, Volkow ND, et al. Graphical analysis of reversible radioligand binding from time-activity measurements applied to [N-^{11}C-methyl]-(−)-cocaine PET studies in human subjects. J Cereb Blood Flow Metab 1990;10:740–747.
21. Logan J, Fowler AH, Volkow ND, et al. Distribution volume ratios without blood sampling from graphical analysis of PET data. J Cereb Blood Flow Metab 1996;16:834–840.
22. Gjedde A. High- and low-affinity transport of D-glucose from blood to brain. J Neurochem 1981;36:1463–1471.
23. Patlak CS, Blasberg RG, Fenstermacher JD. Graphical evaluation of blood-to-brain transfer constants from multiple-time uptake data. J Cereb Blood Flow Metab 1983;3:1–7.
24. Patlak CS, Blasberg RG. Graphical evaluation of blood-to-brain transfer constants from multiple- time uptake data. Generalizations. J Cereb Blood Flow Metab 1985;5:584–590.
25. Thal DR, Rub U, Orantes M, et al. Phases of A beta-deposition in the human brain and its relevance for the development of AD. Neurology 2002;58:1791–1800.
26. Arnold SE, Hyman BT, Flory J, et al. The topographical and neuroanatomical distribution of neurofibrillary tangles and neuritic plaques in the cerebral cortex of patients with Alzheimer's disease. Cereb Cortex 1991;1:103–116.
27. Wolf DS, Gearing M, Snowdon DA, et al. Progression of regional neuropathology in Alzheimer disease and normal elderly: findings from the Nun study. Alzheimer Dis Assoc Disord 1999;13:226–231.
28. Brilliant MJ, Elble RJ, Ghobrial M, et al. The distribution of amyloid beta protein deposition in the corpus striatum of patients with Alzheimer's disease. Neuropathol Appl Neurobiol 1997;23:322–325.
29. Suenaga T, Hirano A, Llena JF, et al. Modified Bielschowsky stain and immunohistochemical studies on striatal plaques in Alzheimer's disease. Acta Neuropathol 1990;80:280–286.
30. Braak H, Braak E. Alzheimer's disease: striatal amyloid deposits and neurofibrillary changes. J Neuropathol Exp Neurol 1990; 49:215–224.
31. Friedland RP, Budinger TF, Ganz E, et al. Regional cerebral metabolic alterations in dementia of the Alzheimer type: positron emission tomography with [18F]fluorodeoxyglucose. J Comput Assist Tomogr 1983;7:590–598.
32. Jelic V, Nordberg A. Early diagnosis of Alzheimer disease with positron emission tomography. Alzheimer Dis Assoc Disord 2000;14(suppl 1):S109–S113.
33. Silverman DH, Small GW, Chang CY, et al. Positron emission tomography in evaluation of dementia: regional brain metabolism and long-term outcome. JAMA 2001;286:2120–2127.
34. Alexander GE, Chen K, Pietrini P, et al. Longitudinal PET evaluation of cerebral metabolic decline in dementia: a potential outcome measure in Alzheimer's disease treatment studies. Am J Psychiatry 2002;159:738–745.
35. Braak H, Braak E. Neuropathological staging of Alzheimer-related changes. Acta Neuropathol 1991;82:239–259.
36. Lewis DA, Campbell MJ, Terry RD, et al. Laminar and regional distributions of neurofibrillary tangles and neuritic plaques in Alzheimer's disease: a quantitative study of visual and auditory cortices. J Neurosci 1987;7:1799–1808.
37. Matsuda H. Cerebral blood flow and metabolic abnormalities in Alzheimer's disease. Ann Nucl Med 2001;15:85–92.
38. Styren SD, Hamilton RL, Styren GC, et al. X-34, a fluorescent derivative of Congo red: a novel histochemical stain for Alzheimer's disease pathology. J Histochem Cytochem 2000;48: 1223–1232.

39. Morris JC, Storandt M, McKeel DW Jr, et al. Cerebral amyloid deposition and diffuse plaques in "normal" aging: evidence for presymptomatic and very mild Alzheimer's disease. Neurology 1996;96:707–719.
40. Goldman WP, Price JL, Storandt M, et al. Absence of cognitive impairment or decline in preclinical Alzheimer's disease. Neurology 2001;56:361–367.
41. Morris JC, Price AL. Pathologic correlates of nondemented aging, mild cognitive impairment, and early-stage Alzheimer's disease. J Mol Neurosci 2001;17:101–118.
42. Schmitt FA, Davis DG, Wekstein DR, et al. "Preclinical" AD revisited: neuropathology of cognitively normal older adults. Neurology 2000;55:370–376.
43. Small GW, Mazziotta JC, Collins MT, et al. Apolipoprotein E type 4 allele and cerebral glucose metabolism in relatives at risk for familial Alzheimer disease. JAMA 1995; 273:942–947.
44. Reiman EM, Caselli RJ, Yun LS, et al. Preclinical evidence of Alzheimer's disease in persons homozygous for the epsilon 4 allele for apolipoprotein E. N Engl J Med 1996;96: 752–758.
45. Kennedy AM, Frackowiak RS, Newman SK, et al. Deficits in cerebral glucose metabolism demonstrated by positron emission tomography in individuals at risk of familial Alzheimer's disease. Neurosci Lett 1995;186:17–20.
46. Wahlund LO, Basun H, Almkvist O, et al. A follow-up study of the family with the Swedish APP 670/671 Alzheimer's disease mutation. Dement Geriatr Cogn Disord 1999;10: 526–533.
47. Ohm TG, Kirca M, Bohl J, et al. Apolipoprotein E polymorphism influences not only cerebral senile plaque load but also Alzheimer-type neurofibrillary tangle formation. Neuroscience 1995;66:583–587.
48. Pirttila T, Soininen H, Mehta PD, et al. Apolipoprotein E genotype and amyloid load in Alzheimer disease and control brains. Neurobiol Aging 1997;18:121–127.
49. Berg L, McKeel DWJ, Miller JP, et al. Clinicopathologic studies in cognitively healthy aging and Alzheimer's disease: relation of histologic markers to dementia severity, age, sex, and apolipoprotein E genotype. Arch Neurol 1998;55: 326–335.
50. Friedland RP, Kalaria R, Berridge M, et al. Neuroimaging of vessel amyloid in Alzheimer's disease. Ann NY Acad Sci 1997; 826:242–247.
51. Shoghi-Jadid K, Small GW, Agdeppa ED, et al. Localization of neurofibrillary tangles and beta-amyloid plaques in the brains of living patients with Alzheimer disease. Am J Geriatr Psychiatry 2002;10:24–35.
52. Glenner GG. Alzheimer's disease. The commonest form of amyloidosis. Arch Pathol Lab Med 1983;107:281–282.